

ISSN 1335-8871

MEASUREMENT SCIENCE REVIEW



Journal homepage: https://content.sciendo.com

Adaptive Measurement Selection for Scalable Distributed Graph Optimization in Multi-UAV Relative Positioning

Chengsong Xiong*⁶, Zheng You

Department of Precision Instrument, Tsinghua University, Beijing, 100084, China xcs20@mails.tsinghua.edu.cn, yz-dpi@mail.tsinghua.edu.cn

Abstract: Autonomous relative positioning is a critical challenge for unmanned aerial vehicle (UAV) swarms. In this study, we address the optimization of measurement constraint selection in the distributed relative positioning process of large-scale UAV swarms. We introduce a distributed graph optimization (DGO) scheme for swarm relative positioning, which enables global consistent relative position estimation through limited inter-UAV information sharing. To prevent the calculation time from escalating with swarm size, this method allows users to specify the number of relative measurement constraints used in the calculation. Building on the Cramér-Rao Lower Bound (CRLB) and Fisher Information Matrix (FIM) theory, we further propose a theoretically optimal method for selecting relative measurement constraints. Different from traditional distributed optimization methods that use fixed constraints, the proposed method can adaptively select the most theoretically advantageous constraints to improve accuracy, resulting in higher precision and improved adaptability to dynamic environments. To validate the effectiveness of the proposed method, we conducted numerical experiments with different swarm sizes and sensing error conditions. The results show that the proposed method has higher accuracy and stability compared to self-pose estimation methods and other measurement selection approaches, while having a low computational load. This work represents the first attempt to incorporate the FIM into constraint selection for distributed localization of UAV swarms.

Keywords: UAV swarm, distributed graph optimization, Fisher Information Matrix, optimal measurement constraint

1. Introduction

In recent years, unmanned aerial vehicle (UAV) swarms have taken on an increasingly important role in different fields, including emergency rescue [1], smart agriculture [2], and urban traffic [3]. The advantage of using UAV swarms over single UAVs is the ability to perform tasks in a collaborative and parallel manner, thereby improving efficiency. Relative positioning serves as the basis for collaboration between UAVs. Acquiring the coordinates of other cooperative targets is essential for each UAV within the swarm to make coordinated decisions, demonstrating the capacity for swarm intelligence. Existing relative positioning systems for UAV swarms include GPS [4], monocular and binocular vision [5], [6], Ultra-Wideband (UWB) [7], and LiDAR [8], among others. However, methods based on GPS and external ground wireless base stations can become unreliable in complex environments such as forests and urban canyons. Therefore, it is of great importance for research that UAVs in a swarm can perform relative positioning through onboard sensors.

UAVs are capable of carrying different types of sensors for relative measurements, which can be categorized into distance measurement, relative direction measurement, and state estimation depending on the type of measurement values. Due to the limited range and accuracy of individual sensors, the relative positioning issues in UAV swarms require

the collaborative integration of multiple sensors. The classical multi-sensor fusion methods for UAV swarm primarily include the Extended Kalman Filter (EKF) [9] and its variants, such as the Unscented Kalman Filter (UKF) [10] and the Variational Bayesian Extended Kalman Filter (VBEKF) [11]. However, filter-based methods usually require high observability between UAVs. In practice, the limited field of view (FOV) of sensors, such as cameras, poses a challenge for the generalization of filtering methods to large-scale swarms. To overcome these limitations, researchers have proposed optimization-based cooperative localization methods for swarms. The mainstream approach is to use UWB modules for distance measurement, deploy cameras for relative direction measurement, and fuse these data with the onboard visual-inertial odometry (VIO) systems through an optimization-based backend [12]. This method effectively addresses the limitations of filter-based methods; however, increasing the scale of the swarm leads to a rapid increase in computational load, which is an urgent issue that needs to be addressed in practical applications. In this context, researchers have proposed distributed optimization approaches, using partial measurement constraints within the swarm instead of global information [13], [14], [15]. In this mechanism, identifying the optimal measurement constraints for optimization is crucial to achieve a balance between compu-

DOI: 10.2478/msr-2025-0023

tational complexity and accuracy. The effect of each pair of measurement constraints on relative positioning accuracy depends not only on sensor accuracy, but also on the topology of the swarm and the actual relative positions between the UAVs. These issues are crucial in the distributed relative positioning process of large-scale swarms and are rarely considered in current research. The introduction of the Fisher Information Matrix (FIM) and the Cramér-Rao Lower Bound (CRLB) theory could be a promising approach to solve this problem [16]. Fisher information is a measure of the expected amount of information about an unknown parameter that a single observation can provide. It can be used to predict the quality of sensor data and has already been applied to localization and topology optimization problems in wireless ground sensor networks [17], [18]. However, its integration with collaborative localization for UAV swarms has received limited attention in previous research.

In this work, we propose a distributed relative positioning method for UAV swarms that adaptively selects the optimal measurement constraints in the computational process. Firstly, using the inter-UAV relative distance measurements, the relative angle measurements, and the self-pose estimation results of each UAV, we formulate a distributed graph optimization (DGO) problem based on graph theory for swarm relative positioning. To evaluate the quality of the onboard sensor data, we introduce FIM and the CRLB theory. This approach allows us to identify the sensor data that are most beneficial for improving relative positioning accuracy from a multitude of measurement constraints. Finally, the selected data are used for swarm relative positioning. We have developed a UAV swarm model and validated the effectiveness of the proposed method using simulation data. The results show that our method achieves theoretically optimal accuracy in the distributed optimization process compared to selecting fixed pairs of measurement constraints or randomly selecting measurement constraints, particularly in scenarios where the swarm topology is complex or undergoes dynamic changes. The proposed method represents the first attempt to incorporate FIM in the constraint selection for distributed graph optimization-based localization in UAV swarms, and contributes to improving the accuracy and real-time performance of relative positioning. This work lays the foundation for further collaborative swarm control and planning missions.

2. DISTRIBUTED RELATIVE POSITIONING FOR UAV SWARMS WITH OPTIMAL MEASUREMENT SELECTION

This study addresses the relative positioning problem between UAVs, independent of ground anchors or satellite bases. As shown in Fig. 1 (a), most existing studies use external wireless nodes to determine the positions of UAVs [19], [20], which limits their flight capabilities to the coverage areas of these nodes. Moreover, any interference in the communication between the nodes and the UAVs in complex environments can lead to failure in positioning. To improve the autonomy of UAV swarms, the relative positioning between UAVs has attracted increasing research interest, as shown in Fig. 1 (b). The relative positioning accuracy depends not only on the sensor errors and algorithms, but also on the formation

configuration of the UAVs. Fig. 1 (c) shows two examples: one shows a swarm formation that facilitates relative position calculation, and the other shows a formation that is unsuitable for such calculations.

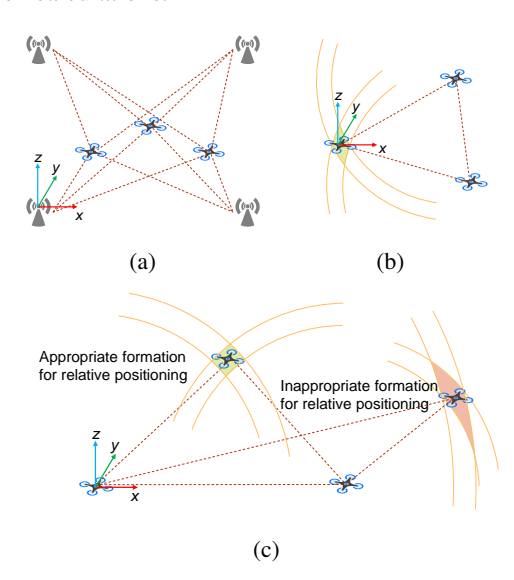


Fig. 1. Schematic diagram of relative positioning for UAV swarm. (a) Positioning based on external anchors. (b) Anchor-free relative positioning. (c) The influence of formation on positioning accuracy.

In the relative positioning problem of large-scale UAV swarms, we found that using the full measurement data to calculate the relative positions is computationally expensive and time-consuming. To overcome this limitation, we have developed an innovative distributed computing architecture that intelligently selects optimal measurement constraints from the swarm's sensor data. In this context, the term "optimal" refers to the selection of an optimal subset of a predetermined size from the entire sensor data set, such that the selected subset minimizes the relative positioning error while maintaining the specified subset size constraint. This advanced approach not only significantly reduces the computation time but also improves the mutual positioning accuracy through its adaptive constraint selection mechanism. In the following sections, we provide a comprehensive description of our proposed methodology.

A. Distributed graph optimization for relative positioning

In this section, we introduce the DGO mechanism for cooperative relative positioning of UAV swarms, as shown in Fig. 2. The UAV swarm is modeled as a mathematical graph G=(V,E), where the set of vertices V in the graph represents the collection of UAV position vectors, and the set of edges E in the graph represents the measurement constraints between the UAVs, including distance measurement constraints, angle measurement constraints, and state estimation constraints. By decomposing the overall topology of the swarm into multiple subgraphs, distributed optimization computations can be performed locally on each UAV platform. By sharing the local calculation results through inter-UAV communication, this approach improves the computational efficiency while ensuring the accuracy of the results.

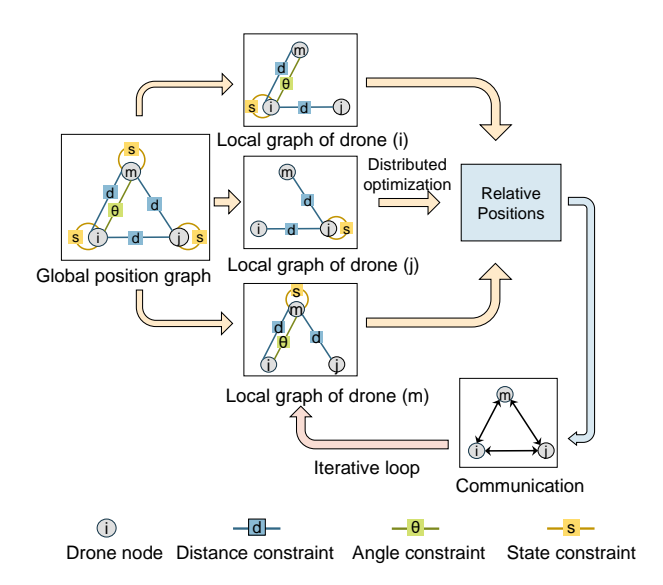


Fig. 2. The DGO scheme for UAV swarm.

The process of DGO is described as follows. Consider a swarm with N UAVs, whose position set is denoted by $\mathbf{P} = \{\mathbf{p}_1, \mathbf{p}_2, \cdots, \mathbf{p}_N\}$. Let $d_{i,j}^m$ be the measured distance between UAV i and UAV j $(i, j \le N)$, which follows a Gaussian distribution:

$$d_{i,j}^{m} = h^{d}\left(\mathbf{p}_{i}, \mathbf{p}_{j}\right) + \mathbf{N}\left(0, \Sigma_{d}^{2}\right) \tag{1}$$

where h^d is the distance measurement function, and Σ_d^2 is the variance of the Gaussian error. In real-world systems, inter-UAV relative ranging is typically based on onboard UWB nodes, which enables anchor-free and omnidirectional distance measurements.

Furthermore, let $\theta_{i,j}^m$ be the measured relative angle between UAV i and UAV j $(i, j \le N)$, and we have

$$\theta_{i,i}^{m} = h^{\theta} \left(\mathbf{p}_{i}, \mathbf{p}_{i} \right) + \mathbf{N} \left(0, \Sigma_{\theta}^{2} \right) \tag{2}$$

where h^{θ} is the angle measurement function, and Σ_{θ}^2 is the variance of the Gaussian error. Relative angle measurements are usually performed by onboard vision systems. However, due to the limited FOV of cameras, a single UAV may have difficulty observing all cooperative targets if the number of UAVs in the swarm is large. Consequently, $\theta_{i,j}$ may not exist between each pair of UAV i and j in the swarm.

In general, UAVs are equipped with pose estimation systems for single-unit attitude control. Let \mathbf{p}_i^s be the position of UAV i obtained from the state estimation system:

$$\mathbf{p}_{i}^{s} = h^{s}\left(\mathbf{p}_{i}\right) + \mathbf{N}\left(\mathbf{0}, \Sigma_{s}^{2}\right) \tag{3}$$

where h^s is the state measurement function, and Σ_s^2 is the variance of the Gaussian error. Although the pose estimation system can directly determine the position of the UAV, the estimation error may increase with time and flight distance. This is because pose estimation systems usually rely on inertial sensors and measurement methods, such as inertial measurement units (IMU), optical flow, and VIO. The process of integrating acceleration and velocity measurements can lead to an accumulation of errors. For swarm relative positioning, inter-UAV relative measurements are required to correct for the drift between the individual UAVs.

Based on the aforementioned measurements, a distributed optimization problem for swarm relative positioning can be formulated. In the distributed scheme, each UAV in the swarm (UAV i) considers its own position \mathbf{p}_i as the unknown variable to be optimized. We define the distance cost function for UAV i as J_i^d , which can be expressed as

$$J_i^d = \sum_{j \in \mathbf{O}_i^d} \left\| d_{i,j}^m - \left\| \mathbf{p}_i - \hat{\mathbf{p}}_j \right\|_2 \right\|_{\Sigma_d}^2$$
 (4)

where \mathbf{O}_i^d is a set of UAV indices. If the distance measurement value between UAV i and UAV j is used in the optimization, then index j is stored in \mathbf{O}_i^d . $\hat{\mathbf{p}}_j$ is the position of UAV j estimated by its local distributed optimization. We assume that UAV i can also determine $\hat{\mathbf{p}}_j$ through inter-UAV communication and use it for its local optimization. The detailed information exchange and iterative process can be found in our previous work [21].

The relative angle cost function for UAV i is defined as J_i^{θ} , which is given by

$$J_i^{\theta} = \sum_{j \in \mathbf{O}_i^{\theta}} \left\| \theta_{i,j}^m - \angle \left(\mathbf{p}_i, \hat{\mathbf{p}}_j \right) \right\|_{\Sigma_{\theta}}^2 \tag{5}$$

where $\angle(\cdot,\cdot)$ represents the relative angle operator. The set \mathbf{O}_i^{θ} represents the index set of cooperative targets that can be observed by UAV i.

Similarly, we define the cost function for state estimation as follows:

$$J_i^s = \|\mathbf{p}_i - \mathbf{p}_i^s\|_{\Sigma_s}^2 \tag{6}$$

Based on (4)-(6), we formulate the distributed optimization problem as follows:

$$\hat{\mathbf{p}}_i = \arg\min_{\mathbf{p}_i} \left(k_d J_i^d + k_\theta J_i^\theta + k_s J_i^s \right) \tag{7}$$

where $\hat{\mathbf{p}}_i$ is the estimated position of UAV i. k_d , k_θ and k_s are user-defined weighting coefficients. In previous research, the method for optimal weight selection was analyzed based on the CRLB and Bayes' theorem. The results show that theoretically optimal performance can be achieved when the weights are inversely proportional to the variances. The weighting coefficients can be dynamically adjusted based on the variances.

After optimization, each UAV shares its estimated local position with other UAVs via inter-UAV communication so that all UAVs can acquire the relative positions of cooperative targets at each time step.

For small-scale swarms, each UAV can perform a DGO with the relative measurement results of all other cooperative targets. In our previous work, we conducted experiments on DGO in a 4-UAV swarm and demonstrated the effectiveness of the proposed method [21]. However, when the swarm size is large, it is necessary to select a limited number of suitable measurement conditions for computation due to the limited sensing capabilities and computational power of a single UAV. More specifically, the swarm must be able to adaptively adjust \mathbf{O}_i^d and \mathbf{O}_i^θ in (4) and (5) based on the swarm topology and sensing accuracy to balance inter-location precision and computational efficiency. The proposed measurement constraint selection method is presented in the following section.

B. Determination of optimal measurement constraints based on FIM

First, we give the definitions of the FIM and the CRLB. Suppose $\mathbf{y} \in \mathbb{R}^q$ is continuous random variable that depends on $\mathbf{x} \in \mathbb{R}^n$. The FIM is given by

$$\mathbf{FIM}(\mathbf{x}) = \mathbb{E}\left[\left(\frac{\partial \ln p\left(\mathbf{y}|\mathbf{x}\right)}{\partial \mathbf{x}}\right)^{T} \left(\frac{\partial \ln p\left(\mathbf{y}|\mathbf{x}\right)}{\partial \mathbf{x}}\right)\right]$$
(8)

where $\mathbb{E}[\cdot]$ is the expectation operator and $p(\cdot)$ is the probability density function. We define $\hat{\mathbf{x}}(\mathbf{y})$ as an unbiased estimator of \mathbf{x} ; therefore, we have

$$\mathbb{E}\left[\mathbf{e}\left(\mathbf{x}\right)\right] = \mathbb{E}\left[\hat{\mathbf{x}}\left(\mathbf{y}\right) - \mathbf{x}\right] = \mathbf{0} \tag{9}$$

According to the Cramér-Rao theorem, the following inequality holds:

$$\operatorname{Cov}\left[\hat{\mathbf{x}}\left(\mathbf{y}\right)\right] = \mathbb{E}\left[\mathbf{e}\left(\mathbf{x}\right)\mathbf{e}\left(\mathbf{x}\right)^{T}\right] \ge \mathbf{CRLB}\left(\mathbf{x}\right)$$
 (10)

where $Cov[\hat{\mathbf{x}}(\mathbf{y})]$ denotes the covariance of $\hat{\mathbf{x}}(\mathbf{y})$, and $CRLB(\mathbf{x})$ is the Cramér-Rao Bound matrix, which can be given by

$$\mathbf{CRLB}(\mathbf{x}) = \mathbf{FIM}(\mathbf{x})^{-1} \tag{11}$$

Let \mathbf{x} be the set of state vectors related to swarm relative positioning, while \mathbf{y} denotes the set of measurement values. According to the Gaussian noise model, we have

$$\mathbf{y} = h(\mathbf{x}) + \mathbf{v}, \mathbf{v} \sim N(\mathbf{0}, \mathbf{R}) \tag{12}$$

Then, the FIM can be given by

$$\mathbf{FIM}(\mathbf{x}) = \mathbf{H}(\mathbf{x})^T \mathbf{R}^{-1} \mathbf{H}(\mathbf{x}) \tag{13}$$

where $\mathbf{H}(\mathbf{x}) = \partial h(\mathbf{x})/\partial \mathbf{x}$. Let $\mathbf{x}_i = [x_i, y_i]^T$ be the state vector of UAV *i*. Considering the measurement between UAV *i* and UAV *j*, let $\mathbf{y}_{i,j} = \left[d_{i,j}^m, \theta_{i,j}^m\right]^T$ be the set of relative distance and relative angle measurements between UAV *i* and UAV *j*. The measurement function $h^{ij}(\cdot)$ can be given by

$$h^{ij}(\mathbf{x}_i) = \begin{bmatrix} \sqrt{(x_i - x_j)^2 + (y_i - y_j)^2} \\ \operatorname{atan}\left(\frac{x_i - x_j}{y_i - y_j}\right) \end{bmatrix}$$
(14)

where $atan(\cdot)$ is the arctangent operator. We define $\mathbf{r}_{i,j} = \begin{pmatrix} r_{i,j}^x, r_{i,j}^y \end{pmatrix} = (x_i - x_j, y_i - y_j)$ as the relative state vector between UAV i and UAV j.

Specifically for situations in which the information about the relative distance or relative angle between the UAVs is not available, we have

$$h^{ij}(\mathbf{x}_{i}) = \begin{cases} \begin{bmatrix} \|\mathbf{r}_{i,j}\|_{2} & \operatorname{atan}\left(\frac{x_{i}-x_{j}}{y_{i}-y_{j}}\right) \end{bmatrix}^{T}, & j \in \mathbf{D}_{i} \cap \Theta_{i} \\ \begin{bmatrix} \|\mathbf{r}_{i,j}\|_{2} & 0 \end{bmatrix}^{T}, & j \in \mathbf{D}_{i} - \Theta_{i} \\ \begin{bmatrix} 0 & \operatorname{atan}\left(\frac{x_{i}-x_{j}}{y_{i}-y_{j}}\right) \end{bmatrix}^{T}, & j \in \Theta_{i} - \mathbf{D}_{i} \end{cases}$$

where $\|\mathbf{r}_{i,j}\|_2 = \sqrt{(x_i - x_j)^2 + (y_i - y_j)^2}$ is the 2-norm of $\mathbf{r}_{i,j}$, \mathbf{D}_i is the set of indices of the UAVs capable of performing

relative distance measurements with UAV i, and Θ_i is the set of indices of the UAVs capable of performing relative angle measurements with UAV i. The measurement matrix $\mathbf{H}^{ij}(\mathbf{x}_i)$ can be expressed as

$$\mathbf{H}^{ij}(\mathbf{x}_{i}) = \begin{cases} \begin{bmatrix} \frac{r_{i,j}^{x}}{\|\mathbf{r}_{i,j}\|_{2}} & \frac{r_{i,j}^{y}}{\|\mathbf{r}_{i,j}\|_{2}} \\ \frac{r_{i,j}^{y}}{\|\mathbf{r}_{i,j}\|_{2}^{2}} & \frac{-r_{i,j}^{x}}{\|\mathbf{r}_{i,j}\|_{2}^{2}} \end{bmatrix}, & j \in \mathbf{D}_{i} \cap \Theta_{i} \\ \begin{bmatrix} \frac{r_{i,j}^{x}}{\|\mathbf{r}_{i,j}\|_{2}} & \frac{r_{i,j}^{y}}{\|\mathbf{r}_{i,j}\|_{2}} \\ 0 & 0 \end{bmatrix}, & j \in \mathbf{D}_{i} - \Theta_{i} \end{cases}$$
(16)
$$\begin{bmatrix} 0 & 0 \\ \frac{r_{i,j}^{y}}{\|\mathbf{r}_{i,j}\|_{2}^{2}} & \frac{-r_{i,j}^{x}}{\|\mathbf{r}_{i,j}\|_{2}^{2}} \end{bmatrix}, & j \in \Theta_{i} - \mathbf{D}_{i} \end{cases}$$

We assume that each UAV uses the data from N_o cooperative UAVs for DGO computations. Let \mathbf{O}_i be the set of indices of all UAVs that participate in the local computation of UAV i, along with its own index. Then we define the measurement quality evaluation function for all cooperative targets as

$$F_{i} = \sum_{j \in \mathbf{O}_{i}} -\ln\left(\left|\mathbf{FIM}^{ij}\left(\mathbf{x}_{i}\right)\right|\right) \tag{17}$$

where $|\mathbf{FIM}^{ij}(\mathbf{x}_i)|$ denotes the determinant of the FIM.

Based on the aforementioned FIM computation process, we can identify the optimal constraints for relative positioning from numerous measurement constraints. Let N_i be the set of indices of all UAVs that can perform relative measurements and communicate with UAV i. For a user-defined N_o , we can derive O_i from N_i :

$$\mathbf{O}_i = \underset{\mathbf{O}_i}{\operatorname{arg\,min}} F_i, \mathbf{O}_i \subseteq \mathbf{N}_i \tag{18}$$

Then, we can derive \mathbf{O}_i^d and \mathbf{O}_i^{θ} from \mathbf{O}_i , which are used for the DGO calculations in (6) and lead to the final inter-UAV relative positioning results.

The optimization problem in (18) is a combinatorial optimization task to select a subset of N_o neighbors from the set N_i . Applying a brute-force approach would require evaluating all possible combinations, especially for large-scale swarms. We use a greedy algorithm to solve this problem efficiently. The objective function F_i is an additive sum of individual quality metrics for each neighbor, such that the global minimum can be found by individually minimizing each term. Consequently, a greedy strategy that selects the neighbors with the smallest individual metrics is guaranteed to be optimal. The algorithm proceeds as follows:

- 1) For each candidate neighbor $j \in \mathbb{N}_i$, compute its individual contribution to the objective function using (18).
- 2) Sort all candidate neighbors in N_i in ascending order according to their corresponding metric.
- 3) Select the first N_o neighbors from the sorted list to form the optimal set \mathbf{O}_i .

The overall complexity is the sum of these steps, where the dominant term is the sorting operation. Therefore, the total computational complexity of our measurement selection algorithm is $O(|\mathbf{N}_i|\log(|\mathbf{N}_i|))$. This polynomial-time complexity is highly efficient and ensures that the selection process remains computationally feasible for real-time computation, even as the swarm size increases.

Algorithm 1 DGO with optimal measurements selection based on FIM

Input: Distance measurements $\left\{d_{i,j}^m|j\in\mathbf{D}_i\right\}$, angle measurements $\left\{\theta_{i,j}^m|j\in\Theta_i\right\}$, state estimation \mathbf{p}_i^s , the set of neighbors \mathbf{N}_i , the number of UAVs utilized in the optimization N_o

```
Output: Optimized relative positions \mathbf{P}_{i}^{R}
  1: Initialize system
  2: while system is running do
          for UAV i in swarm S do
  3:
              Obtain \left\{d_{i,j}^{m}|j\in\mathbf{D}_{i}\right\}, \left\{\theta_{i,j}^{m}|j\in\Theta_{i}\right\}, and \mathbf{p}_{i}^{s} from
  4:
              Receive \{\hat{\mathbf{p}}_i | j \in \mathbf{N}_i\} from neighbors in \mathbf{N}_i
  5:
              for j in N_i do
  6:
                  Calculate \mathbf{H}^{ij}(\mathbf{x}_i) using (16)
  7:
  8:
                  Generate FIM<sup>ij</sup> (x) from H<sup>ij</sup> (x<sub>i</sub>) using (13)
              end for
  9.
              Calculate F_i using (17)
 10:
              Optimize \mathbf{O}_i based on (18) and user-defined N_o
11:
              Get \mathbf{O}_i^d and \mathbf{O}_i^{\theta} from \mathbf{O}_i
12:
              Optimize \hat{\mathbf{p}}_i using (4)-(7)
13:
              Calculate the relative positions between UAV i and
 14:
              other UAVs \mathbf{P}_{i}^{R} using \hat{\mathbf{p}}_{i} and \{\hat{\mathbf{p}}_{i}|j\in\mathbf{N}_{i}\}
              UAV i shares \hat{\mathbf{p}}_i to neighbors
15:
          end for
16:
17: end while
```

A key challenge in swarm positioning is that certain topological configurations can affect the system's observability. For example, if multiple UAVs are in a collinear or near-collinear arrangement, their relative measurements can become linearly dependent. This dependence may cause the measurement Jacobian matrix $\mathbf{H}(\mathbf{x})$ to be rank-deficient. Since the FIM is calculated according to (13), a rank-deficient Jacobian leads directly to a singular or near-singular FIM. In such cases, the system becomes unobservable and the CRLB for the positioning error would approach infinity.

However, the FIM-based measurement selection method proposed here contains its own strategy to mitigate this problem. Our objective function in (18) evaluates the quality of each measurement based on the determinant of its corresponding FIM. If a measurement from a candidate neighbor j produces or enhances a degenerate topology, its associated \mathbf{FIM}^{ij} will be near-singular, so that its determinant approaches zero. Consequently, the quality metric for this neighbor, $-\ln(|\mathbf{FIM}^{ij}(\mathbf{x}_i)|)$, approaches positive infinity.

During the optimization described in (18), the proposed algorithm tries to select the N_o neighbors with the smallest

quality metrics. Therefore, the algorithm automatically penalizes and discards measurements that affect the system observability. This ensures that the subgraph selected for the DGO maintains a strong observability, thus improving the robustness and accuracy of the final positioning solution.

Furthermore, the DGO approach cannot guarantee accuracy if the observability is significantly degraded due to changes in the formation topology. In such circumstances, the solution robustness can be improved by dynamically increasing the weighting of the robot's self-pose estimate (which is less affected by the formation changes) within the optimization problem.

The computational process of the proposed method is illustrated in Algorithm 1.

3. RESULTS AND ANALYSIS

A. Simulation setup

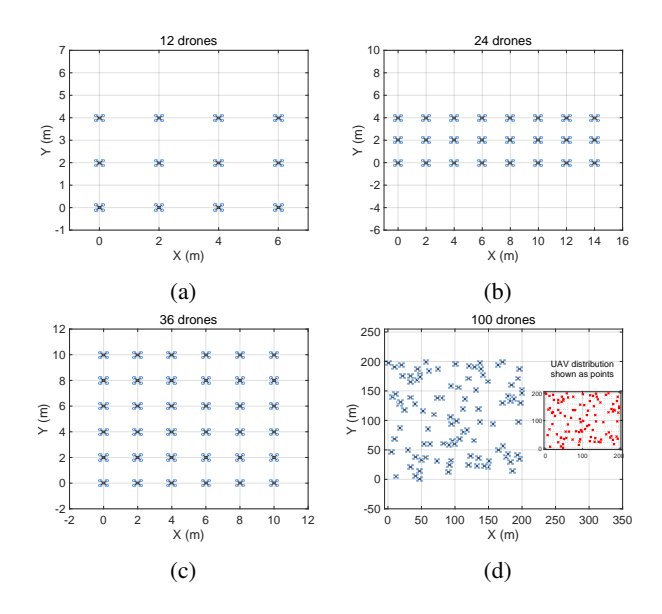


Fig. 3. UAV swarms used in the simulations. (a) 12-UAV swarm. (b) 24-UAV swarm. (c) 36-UAV swarm. (d) 100-UAV swarm.

To evaluate the effectiveness of the proposed method for large-scale UAV swarm relative positioning problems, we conducted numerical experiments, using the proposed FIMbased method to select the optimal measurement constraints for DGO. As shown in Fig. 3, four groups of swarms with different sizes were used, consisting of 12, 24, 36, and 100 UAVs, respectively. In the first three groups of swarms, the UAVs were arranged in a rectangular formation; in the swarm of 100 UAVs, their positions were randomly distributed within a 200 m × 200 m area. Assume the relative measurement errors between the UAVs are: $\Sigma_d = 0.1m$ and $\Sigma_{\theta} = 3^{\circ}$, together with a state estimation error of $\Sigma_{s} =$ 1m. The simulation model was developed using MATLAB R2022b and ran on a computer equipped with an Intel i5-12500H 2.50 GHz processor and 16 GB RAM. The simulation parameters and error characteristics in this section are consistent with the findings from our previous research [21] in real-world scenarios.

In the proposed method, for a given number N_o , we select N_o UAVs from the swarm to participate in the computation process of UAV i by minimizing F_i . Then the relative positions can be solved with DGO. For comparison, we used five other methods to compute the relative positions: 1) state estimation: each UAV computes its position using only its own state estimation system; 2) centralized graph optimization (CGO): a central node collects all measurement data (distance, angle) from each UAV in the swarm and then performs a global graph optimization to compute the relative positions; 3) distributed filtering (DF): each UAV exchanges its state estimate and covariance information with its neighboring nodes to perform prediction, and uses the relative distance and angle measurements to update the steps based on a typical distributed Kalman Filter; 4) DGO-F_i-max: each UAV selects N_o neighbors with the largest F_i values for DGO; 5) DGO- F_i random: each UAV randomly selects N_o neighboring UAVs for the DGO computations.

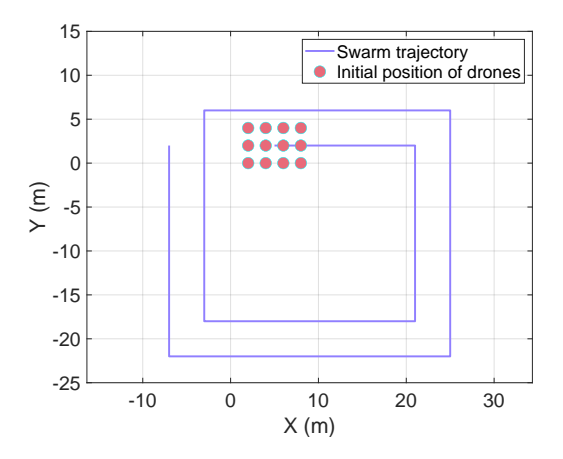


Fig. 4. The flight trajectory of the swarm.

In each simulation group, the UAVs follow a circular trajectory at a constant speed of 1 m/s, traveling a total distance of 100 m. For example, the flight trajectories of the aforementioned 12-UAV swarm are shown in Fig. 4. We varied N_o and analyzed the relative positioning error of the aforementioned methods. For each set of parameters, we use the average error value in the flight process to access the final error size. Define the average relative positioning error of the swarm for each test as follows:

$$MAE = \frac{1}{N} \sum_{i=1}^{N} \|(\hat{\mathbf{p}}_i - \hat{\mathbf{p}}_{cen}) - (\mathbf{p}_i - \mathbf{p}_{cen})\|_2$$
 (19)

where \mathbf{p}_{cen} is the position of the geometric center of the swarm, and $\hat{\mathbf{p}}_{cen}$ is the estimated value of \mathbf{p}_{cen} .

B. Large-scale UAV swarm simulations

The results of the numerical experiments are shown in Fig. 5. It can be observed that the magnitude of the state estimation error remains largely consistent for experiments with different numbers of UAVs and different N_o values. Without correcting the inter-UAV relative positions by relative measurements, the state estimation method cannot be directly applied to swarm localization. The errors of the CGO and DF

methods are smaller compared to the state estimation methods, but they have inherent drawbacks: the DF method converges slowly when the number of nodes is large, and their estimation errors are sensitive to initial values; CGO uses relative measurements between all UAVs in the swarm, but when the number of nodes is large, a high-dimensional optimization problem of dimension 2*N (N is the number of UAVs) must be solved, which is computationally complex, difficult to converge to the optimal solution, and requires extensive inter-UAV information exchange.

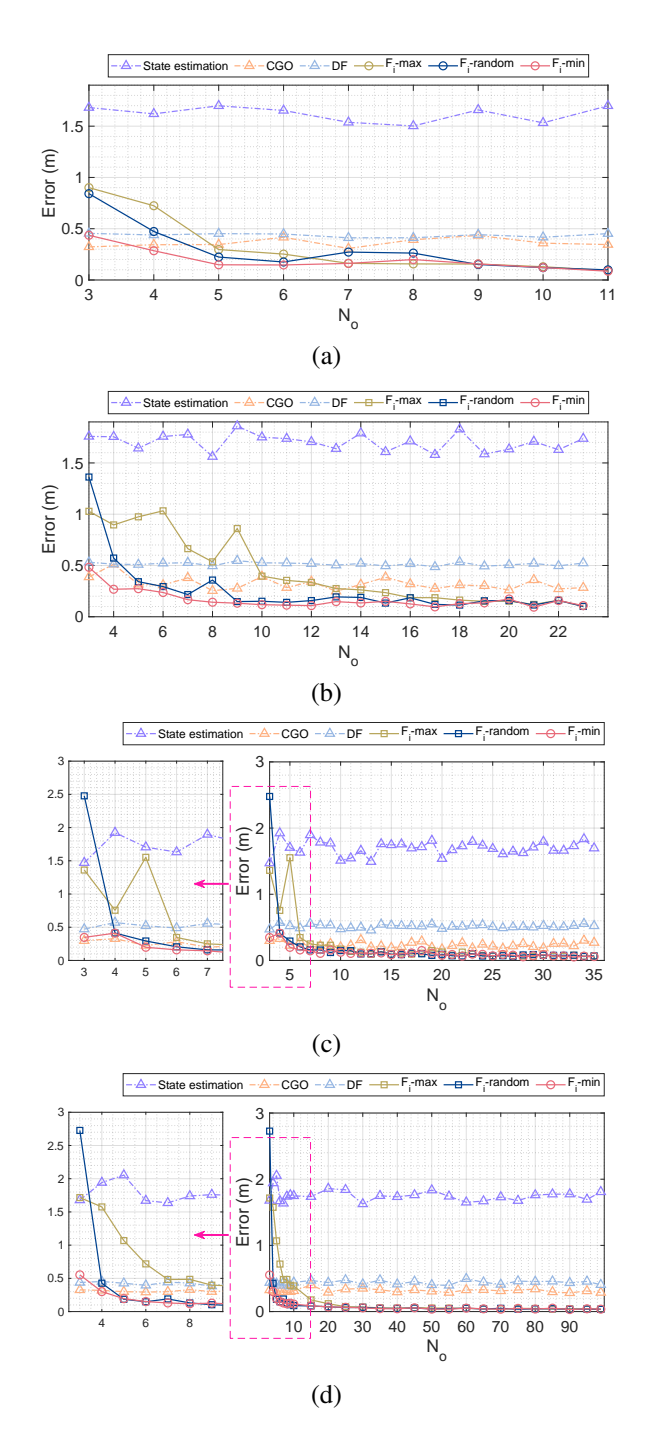


Fig. 5. Relative positioning error variations with respect to N_o across four methods. (a) Error curves for the 12-UAV swarm. (b) Error curves for the 24-UAV swarm. (c) Error curves for the 36-UAV swarm. (d) Error curves for the 100-UAV swarm.

The remaining three DGO-based methods all show a significant corrective effect on the positioning errors, resulting in an lower overall error than that of the state estimation error. Moreover, the errors of the three methods decrease with increasing N_o . Among the methods mentioned above, the method that maximizes F_i has the largest total error. This is due to the negative correlation between F_i and the theoretical error, which indicates that this method includes the least suitable measurement constraints for localization in the calculation process. The total error of the method in which participants are randomly selected for positioning calculations is smaller than that of the F_i -max method. However, for specific values of N_o , e.g. when $N_o = 3$, the error becomes unstable. The observed error fluctuations are due to the stochastic nature of the selection process and its interaction with the swarm's topology. As discussed in Section 2, certain geometric configurations of UAVs can degrade the system's observability. This leads to a rank-deficient Jacobian matrix and consequently a near-singular FIM. By its very nature, the random selection method occasionally and unintentionally selects such ill-conditioned subsets of neighbors.

Among the four methods, the proposed F_i -min method achieves the minimum error and keeps the error constant within 0.5 m across different configurations of swarm size and N_o . This is because the minimization of F_i ensures that the sensor data included in the calculations makes the greatest contribution to improving accuracy. Therefore, this method is highly suitable for distributed calculation scenarios.

Furthermore, we observed the impact of changes in N_o on the localization error. Within the distributed computing framework, increasing N_o improves accuracy but at the cost of higher computational overhead. Therefore, it is important to determine an appropriate value of N_o in order to achieve a balance between accuracy and computational cost. In the four experimental groups shown in Fig. 5, the error of the proposed method decreases significantly with the increase of N_o when $N_o < 10$. Beyond this threshold, the error converges towards the theoretical minimum and stabilizes.

Fig. 6 illustrates the variation in computation time with N_o . Since the dimensions of the variables to be optimized in the proposed DGO computation do not increase with the number of UAVs, the trend in the computation time shows a relatively smooth variation. Consequently, it is justified to set N_o below 10, as this achieves accuracy close to the theoretical minimum while the computational overhead remains low. In particular, the computation time per step remains at around 10 ms—less than half the time required for $N_o = 100$. Meanwhile, the computation time per iteration in CGO increases exponentially with the number of drones, which is significantly higher than the proposed method. When the number of drone agents reaches 100, the single-step computation time on a PC is 3.5 s, indicating that it is difficult to meet the real-time requirements of large-scale swarms in engineering practice.

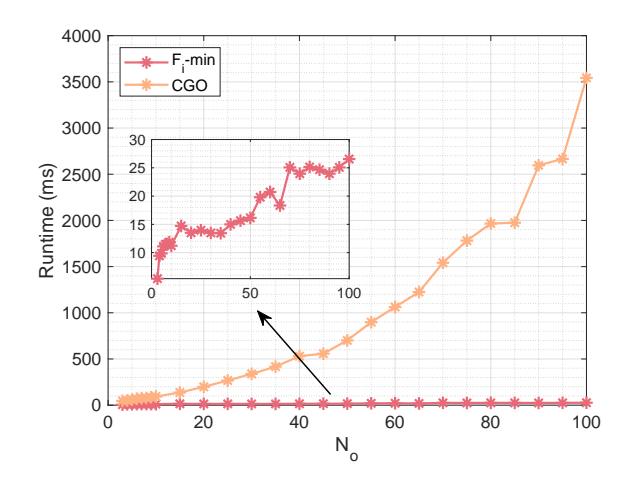


Fig. 6. The variation of computation time per step with N_o .

C. Variable error scenarios

We also investigated the adaptability of the proposed method to different error conditions. For the 100-UAV swarm with configurations of N_o =4, 6, 8, and 10, the parameter pairs $(\Sigma_d, \Sigma_\theta)$ were assigned values of (0.1 m, 3°), (0.2 m, 6°), (0.3 m, 9°), and (0.4 m, 12°), respectively. Comparative localization errors of the four methods under these heterogeneous error conditions are shown quantitatively in Fig. 7. The results show that the localization errors of the three relative positioning methods progressively increase with increasing sensing errors. However, the proposed method consistently shows significantly lower localization errors under different error conditions, confirming its adaptability to heterogeneous error scenarios. In practical applications, the proposed method is expected to demonstrate robust adaptability for UAVs with different sensing hardware.

D. Dynamic swarm formation reconfiguration

To evaluate the robustness of the proposed method under different UAV swarm formation topologies, we conducted a simulation experiment for dynamic formation reconfiguration. As shown in Fig. 8, a 24-UAV swarm was used to successively transition from a rectangle formation to a circular formation and then to a V-formation. The entire reconfiguration process lasted 100 seconds. During the transformation, the relative positioning error of the swarm was calculated using the six aforementioned methods.

As shown in Fig. 9, the error trajectories during the dynamic topology reconfiguration show a remarkable increase in magnitude compared to the static topology cases. Moreover, the errors exhibit a certain degree of random walk behavior due to the frequent communication disruptions and formation adjustments in dynamic environments.

As the simulation results show, the proposed method adaptively selects the optimal constraints in dynamic topology changes, which significantly reduces the average localization error. Table 1 summarizes the statistical metrics (mean absolute error (MAE), standard deviation (STD), and maximum error (MAX)) of the six methods, which further confirm the robustness of the proposed approach in dynamic environments.

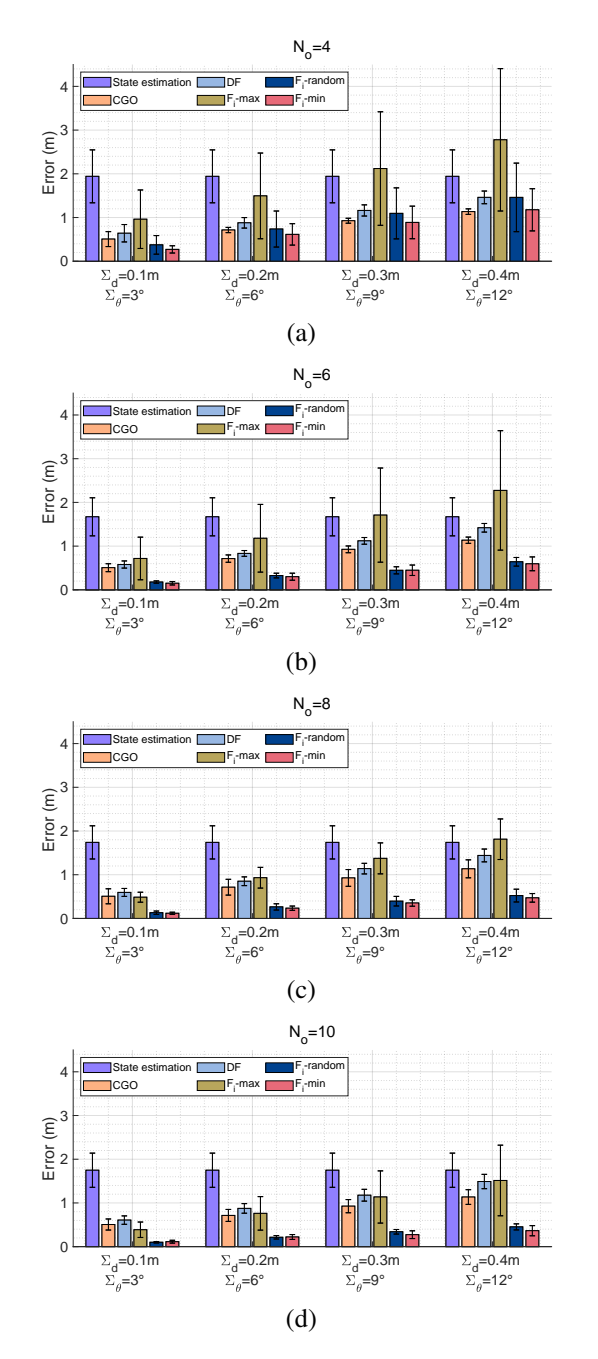


Fig. 7. Relative positioning error for four methods in the 100-UAV swarm under different sensing conditions. (a) $N_o = 4$. (b) $N_o = 6$. (c) $N_o = 8$. (d) $N_o = 10$.

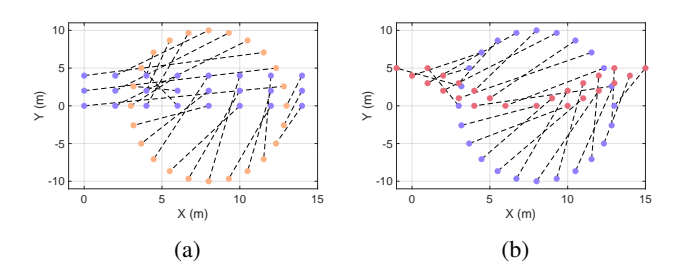


Fig. 8. Dynamic formation reconfiguration. (a) Transformation from rectangle formation to circular formation. (b) Transformation from circular formation to V-formation.

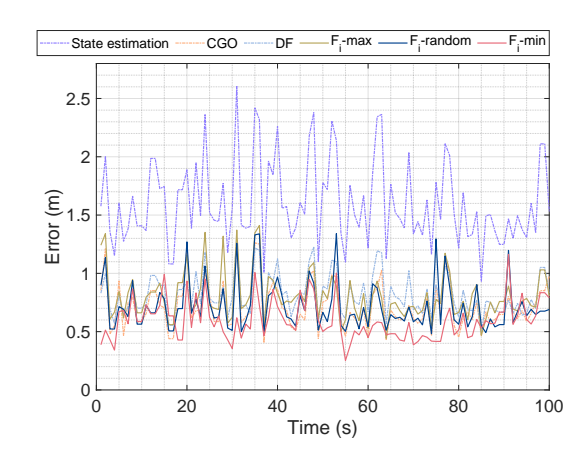


Fig. 9. Error curves in topology reconfiguration simulation.

Table 1. The statistical metrics of the relative positioning methods.

Method	MAE (m)	STD (m)	MAX (m)
State estimation	1.605	0.365	2.606
CGO	0.718	0.200	1.276
DF	0.818	0.179	1.286
F_i -max	0.803	0.206	1.410
F _i -random	0.720	0.213	1.340
F_i -min	0.599	0.169	1.163

We recognize the importance of overcoming real-world communication challenges. In our DGO-FIM framework, the UAVs use the last received positions of their neighbors for local optimization. Communication delays and packet loss in real-world scenarios lead to outdated position data and thus to errors that affect the swarm positioning accuracy during maneuvers. A possible solution to compensate for time-delay errors is to integrate the inertial state estimates (prediction) of the UAVs with the DGO results (measurements) using time-delay Kalman filtering [21]. This multi-method integration increases system stability.

4. CONCLUSIONS

In this paper, we investigate the issue of selecting appropriate relative sensor data for computation in the context of distributed relative positioning in large-scale UAV swarms to improve accuracy while keeping the computational load low. First, we propose a DGO method to calculate the relative positions within the swarm. Then, based on CRLB and FIM theory, we establish a criterion for selecting UAVs participating in the computation when the number of neighboring UAVs involved in the distributed computation is fixed for each UAV. This criterion is determined by considering the swarm's topological structure and the accuracy of the relative measurements. Finally, we show through numerical experiments that the proposed method effectively corrects the drift in the state estimation systems of large-scale UAV swarms. The achieved relative positioning accuracy of the swarm is very close to the theoretical optimum compared to other measurement data selection methods. Our method achieves a computation time of less than 30 ms for up to 100 UAVs, thus meeting the time requirement for commercial micro-UAV autopilots. The approach can be extended to include heterogeneous sensors.

REFERENCES

- [1] Sun, G., He, L., Sun, Z., Wu, Q., Liang, S., Li, J., Niyato, D., Leung, V. C. (2024). Joint task offloading and resource allocation in aerial-terrestrial UAV networks with edge and fog computing for post-disaster rescue. *IEEE Transactions on Mobile Computing*, 23 (9), 8582–8600. https://doi.org/10.1109/TMC.2024.3350886.
- [2] Maddikunta, P. K. R., Hakak, S., Alazab, M., Bhattacharya, S., Gadekallu, T. R., Khan, W. Z., Pham, Q.-V. (2021). Unmanned aerial vehicles in smart agriculture: Applications, requirements, and challenges. *IEEE Sensors Journal*, 21 (16), 17608–17619. https://doi.org/10.1109/JSEN.2021.3049471.
- [3] Liu, B., Zhang, W., Chen, W., Huang, H., Guo, S. (2020). Online computation offloading and traffic routing for UAV swarms in edge-cloud computing. *IEEE Transactions on Vehicular Technology*, 69 (8), 8777–8791. https://doi.org/10.1109/TVT.2020.2994541.
- [4] Irfan, M., Dalai, S., Trslic, P., Santos, M. C., Riordan, J., Dooly, G. (2024). LGVINS: LiDAR-GPS-visual and inertial system based multi-sensor fusion for smooth and reliable UAV state estimation. *IEEE Transactions on Intelligent Vehicles*. https://doi.org/10.1109/TIV.2024.3469551.
- [5] Choutri, K., Lagha, M., Meshoul, S., Shaiba, H., Chegrani, A., Yahiaoui, M. (2024). Vision-based UAV detection and localization to indoor positioning system. *Sensors*, 24 (13), 4121. https://doi.org/10.3390/ s24134121.
- [6] Teixeira, L., Maffra, F., Moos, M., Chli, M. (2018). VI-RPE: Visual-inertial relative pose estimation for aerial vehicles. *IEEE Robotics and Automation Letters*, 3 (4), 2770–2777. https://doi.org/10.1109/ LRA.2018.2837687.
- [7] Yang, X., Wang, J., Song, D., Feng, B., Ye, H. (2021). A novel NLOS error compensation method based IMU for UWB indoor positioning system. *IEEE Sensors Journal*, 21 (9), 11203–11212. https://doi.org/10.1109/JSEN.2021.3061468.
- [8] Wallace, L., Lucieer, A., Watson, C., Turner, D. (2012). Development of a UAV-LiDAR system with application to forest inventory. *Remote sensing*, 4 (6), 1519–1543. https://doi.org/10.3390/rs4061519.
- [9] Wu, Y., Guadagnino, T., Wiesmann, L., Klingbeil, L., Stachniss, C., Kuhlmann, H. (2024). LIO-EKF: High frequency LiDAR-inertial odometry using extended Kalman filters. In 2024 IEEE International Conference on Robotics and Automation (ICRA). IEEE, 13741–13747. https://doi.org/10.1109/ ICRA57147.2024.10610667.

- [10] Tang, X., Yang, L., Wang, D., Li, W., Xin, D., Jia, H. (2025). A collaborative navigation algorithm for UAV Ad Hoc network based on improved sequence quadratic programming and unscented Kalman filtering in GNSS denied area. *Measurement*, 242, 115977. https://doi.org/10.1016/j. measurement.2024.115977.
- [11] Qiu, Z., Wang, S., Hu, P., Guo, L. (2024). Outlier-robust extended Kalman filtering for bioinspired integrated navigation system. *IEEE Transactions on Automation Science and Engineering*, 21 (4), 5881–5894. https://doi.org/10.1109/TASE.2023.3319508.
- [12] Xu, H., Zhang, Y., Zhou, B., Wang, L., Yao, X., Meng, G., Shen, S. (2022). Omni-swarm: A decentralized omnidirectional visual-inertial-UWB state estimation system for aerial swarms. *IEEE Transactions on Robotics*, 38 (6), 3374–3394. https://doi.org/10.1109/TRO.2022.3182503.
- [13] Ziegler, T., Karrer, M., Schmuck, P., Chli, M. (2021). Distributed formation estimation via pairwise distance measurements. *IEEE Robotics and Automation Letters*, 6 (2), 3017–3024. https://doi.org/10.1109/LRA.2021.3062347.
- [14] Horyna, J., Baca, T., Walter, V., Albani, D., Hert, D., Ferrante, E., Saska, M. (2023). Decentralized swarms of unmanned aerial vehicles for search and rescue operations without explicit communication. *Autonomous Robots*, 47 (1), 77–93. https://doi.org/10.1007/s10514-022-10066-5.
- [15] Yang, P., Ye, G.-Y., Shao, C.-L., Yang, S.-L., Huang, Z.-X. (2024). A distributed factor graph model solving method for cooperative localization of UAV swarms. *Measurement Science and Technology*, 36 (1), 016326. https://doi.org/10.1088/1361-6501/ad91d6.
- [16] Cano, J., Pages, G., Chaumette, E., Le Ny, J. (2022). Optimal localizability criterion for positioning with distance-deteriorated relative measurements. In 2022 IEEE/RSJ International Conference on Intelligent Robots and Systems (IROS). IEEE, 947–953. https://doi.org/10.1109/IROS47612.2022.9981718.
- [17] Rui, Y., Zhu, C., Chen, J., Zhou, Z., Pu, Y. (2024). Study on sensor network optimization for MS/AE monitoring system using fisher information and improved encoding framework. *IEEE Sensors Journal*, 24 (14). https://doi.org/10.1109/JSEN.2024.3383864.
- [18] Kim, S.-H., Cho, C. (2024). Effective independence in optimal sensor placement associated with general fisher information involving full error covariance matrix. *Mechanical Systems and Signal Processing*, 212, 111263. https://doi.org/10.1016/j.ymssp.2024.111263.
- [19] Ni, H., Zhu, Q., Hua, B., Mao, K., Pan, Y., Ali, F., Zhong, W., Chen, X. (2024). Path loss and shadowing for UAV-to-ground UWB channels incorporating the effects of built-up areas and airframe. *IEEE Transactions on Intelligent Transportation Systems*, 25 (11), 17066–17077. https://doi.org/10.

1109/TITS.2024.3418952.

- [20] Zhang, K., Chen, P., Ma, T., Gao, S. (2022). Ondemand precise tracking for energy-constrained UAVs in underground coal mines. *IEEE Transactions on Instrumentation and Measurement*, 71, 5500814. https://doi.org/10.1109/TIM.2022.3146925.
- [21] Xiong, C., Lu, W., Xiong, H., Ding, H., He, Q., Zhao, D., Wan, J., Xing, F., You, Z. (2024).

Onboard cooperative relative positioning system for Micro-UAV swarm based on UWB/Vision/INS fusion through distributed graph optimization. *Measurement*, 234, 114897. https://doi.org/10.1016/j.measurement.2024.114897.

Received March 2, 2025 Accepted July 25, 2025